Inorganic Chemistry
Article

Inorg. Chem. **2010**, *49*, 11415–11420 **11415**
DOI: 10.1021/ic101387c

Anion-Directed Self-Assembly in Coordination Networks: Architectural Control *via* Cooperative Noncovalent Interactions

Behrouz Notash, Nasser Safari,* and Hamid Reza Khavasi

Chemistry Department, Shahid Beheshti University, G. C., Evin, Tehran 1983963113, Iran

Received July 12, 2010

The self-assembly of a new flexible tritopic pyrazine−pyridine ligand (pz-3-py) with HgX_2 (X = Cl, Br) was investigated. The results show that coordinated chloride and bromide anions play different roles, and two architecturally different coordination polymers were obtained with the anions used. Where X = Cl, in $[Hg(\mu_3\text{-pz-3-py})Cl_2]_n$ (**1**), the 2D network is isolated, while for X = Br, in $[Hg(\mu\text{-pz-3-py})Br_2]_n$ (**2**), a 1D zigzag chain is constructed. Our results show that noncovalent interactions such as hydrogen bond, halogen···halogen, and halogen···π interactions, when acting cooperatively, are driving forces for the selection of different structures.

Introduction

Over the past few decades, the crystal engineering of coordination polymers and metallo-supramolecular architectures has been studied extensively due to their structural versatility, unique properties, and applications in different areas of science, such as materials and nanotechnology.[1] Therefore, designing self-assembled coordination polymers and inorganic architectures accompanied by control of the noncovalent interactions,[2] called "*the glue of supramolecular chemistry*", is an active theme nowadays.[3] So, the effects of noncovalent interactions in directing the self-assembly of coordination compounds are valuable to inorganic chemists.[4] More recently, the effects of noncovalent interactions on controlling coordination geometry,[5a,b] the coordination mode of the ligand,[5c−e] and the competition between interactions[5f] and also between the coordination bond and noncovalent interactions[5g] have been studied. Recently, Khavasi and his co-workers showed that noncovalent interactions[5a] and temperature parameters[6] have dramatic effects on geometrical and topological control in mercury coordination

*To whom correspondence should be addressed. E-mail: n-safari@cc.sbu.ac.ir.

(1) (a) Tiekink, E. R. T.; Vittal, J. J. *Frontiers in Crystal Engineering*; John Wiley & Sons: Chichester, U. K., 2006. (b) Braga, D.; Grepioni, F. *Making Crystals by Design, Methods, Techniques and Applications*; Wiley-VCH: Weinheim, Germany, 2007. (c) Batten, S. R.; Neville, S. M.; Turner, D. R. *Coordination Polymers: Design, Analysis and Application*; Royal Society of Chemistry: Cambridge, U. K., 2009. (d) Steed, J. W.; Atwood, J. L. *Supramolecular Chemistry*, 2nd ed.; John Wiley & Sons: Chichester, U. K., 2009.

(2) (a) Jeffrey, G. A. *An Introduction to Hydrogen Bonding*; Oxford University Press: Oxford, U. K., 1997. (b) Janiak, C. *J. Chem. Soc., Dalton Trans.* **2000**, 3885–3896. (c) Schottel, B. L.; Chifotides, H. T.; Dunbar, K. R. *Chem. Soc. Rev.* **2008**, *37*, 68–83. (d) Mooibroek, T. J.; Black, C. A.; Gamez, P.; Reedijk, J. *Cryst.Growth Des.* **2008**, *8*, 1082–1093. (e) Mooibroek, T. J.; Gamez, P.; Reedijk, J. *CrystEngComm* **2008**, *10*, 1501–1515. (f) Egli, M.; Sarkhel, S. *Acc. Chem. Res.* **2007**, *40*, 197–205. (g) Metrangolo, P.; Meyer, F.; Pilati, T.; Resnati, G.; Terraneo, G. *Angew. Chem., Int. Ed.* **2008**, *47*, 6114–6127. (h) Brammer, L.; Espallargas, G. M.; Libri, S. *CrystEngComm* **2008**, *10*, 1712–1727. (i) Nishio, M.; Umezawa, Y.; Honda, K.; Tsuboyama, S.; Suezawa, H. *CrystEngComm* **2009**, *11*, 1757–1788.

(3) (a) Lindoy, L. F.; Atkinson, I. *Self-Assembly in Supramolecular Systems*; Royal Society of Chemistry: Cambridge, U. K., 2000. (b) Wu, X.-T.; *Controlled Assembly and Modification of Inorganic Systems*; Springer: Heidelberg, Germany, 2009. (c) Rehm, T.; Schmuck, C. *Chem. Commun.* **2008**, 801–813.

(4) (a) Kaczorowski, T.; Justyniak, I.; Lipińska, T.; Lipkowski, J.; Lewiński, J. *J. Am. Chem. Soc.* **2009**, *131*, 5393–5395. (b) Lu, J.; Turner, D. R.; Harding, L. P.; Byrne, L. T.; Baker, M. V.; Batten, S. R. *J. Am. Chem. Soc.* **2009**, *131*, 10372–10373. (c) Liang, J.; Wu, B.; Jiaac, C.; Yang, X.-J. *CrystEngComm* **2009**, *11*, 975–977. (d) Chen, C.-L.; Su, C.-Y.; Cai, Y.-P.; Zhang, H.-X.; Xu, A.-W.; Kang, B.-S.; Zur Loye, H.-C. *Inorg. Chem.* **2003**, *42*, 3738–3750. (e) Reger, D. L.; Semeniuc, R. F.; Rassolov, V.; Smith, M. D. *Inorg. Chem.* **2004**, *43*, 537–554. (f) Espallargas, G. M.; Zordan, F.; Marín, L. A.; Adams, H.; Shankland, K.; van de Streek, J.; Brammer, L. *Chem.—Eur. J.* **2009**, *15*, 7555–7568. (g) Dai, F.; He, H.; Zhao, X.; Ke, Y.; Zhang, G.; Sun, D. *CrystEngComm* **2010**, *12*, 337–340.

(5) (a) Khavasi, H. R.; Azizpoor Fard, M. *Cryst. Growth Des.* **2010**, *10*, 1892–1896. (b) Kato, M.; Kojima, K.; Okamura, T.; Yamamoto, H.; Yamamura, T.; Ueyama, N. *Inorg. Chem.* **2005**, *44*, 4037–4044. (c) Kobrsi, I.; Knox, J. E.; Heeg, M. J.; Schlegel, H. B.; Winter, C. H. *Inorg. Chem.* **2005**, *44*, 4894–4896. (d) Ghosh, A. K.; Ghoshal, D.; Zangrando, E.; Ribas, J.; Ray Chaudhuri, N. *Inorg. Chem.* **2005**, *44*, 1786–1793. (e) Ghoshal, D.; Ghosh, A. K.; Ribas, J.; Mostafa, G.; Ray Chaudhuri, N. *CrystEngComm* **2005**, *7*, 616–620. (f) Zordan, F.; Purver, S. L.; Adams, H.; Brammer, L. *CrystEngComm* **2005**, *7*, 350–354. (g) Smart, P.; Espallargas, G. M.; Brammer, L. *CrystEngComm* **2008**, *10*, 1335–1344. (h) Schottel, B. L.; Chifotides, H. T.; Shatruk, M.; Chouai, A.; Pérez, L. M.; Bacsa, J.; Dunbar, K. R. *J. Am. Chem. Soc.* **2006**, *128*, 5895–5912. (i) Campos-Fernández, C. S.; Schottel, B. L.; Chifotides, H. T.; Bera, J. K.; Bacsa, J.; Koomen, J. M.; Russell, D. H.; Dunbar, K. R. *J. Am. Chem. Soc.* **2005**, *127*, 12909–12923. (j) Zhou, H.-P.; Gan, X.-P.; Li, X.-L.; Liu, Z.-D.; Geng, W.-Q.; Zhou, F.-X.; Ke, W.-Z.; Wang, P.; Kong, L.; Hao, F.-Y.; Wu, J.-Y.; Tian, Y.-P. *Cryst.Growth Des.* **2010**, *10*, 1767–1776. (k) Zhou, H.-P.; Yin, J.-H.; Zheng, L.-X.; Wang, P.; Hao, F.-Y.; Geng, W.-Q.; Gan, X.-P.; Xu, G.-Y.; Wu, J.-Y.; Tian, Y.-P.; Tao, X.-T.; Jiang, M.-H.; Kan, Y.-H. *Cryst. Growth Des.* **2009**, *9*, 3789–3798. (l) Kundu, N.; Audhya, A.; Towsif Abtab, S. M.; Ghosh, S.; Tiekink, E. R. T.; Chaudhury, M. *Cryst. Growth Des.* **2010**, *10*, 1269–1282. (m) Manzano, B. R.; A.; Jalón, F.; Soriano, M. L.; Carrión, M. C.; Carranza, M. P.; Mereiter, K.; Rodriguez, A. M.; de la Hoz, A.; Sánchez-Migallón, A. *Inorg. Chem.* **2008**, *47*, 8957–8971.

(6) Khavasi, H. R.; Mir Mohammad Sadegh, B. *Inorg. Chem.* **2010**, *49*, 5356–5358.

Published on Web 11/15/2010

Scheme 1. Synthesis Route and Supramolecular Architecture of **1** and **2**

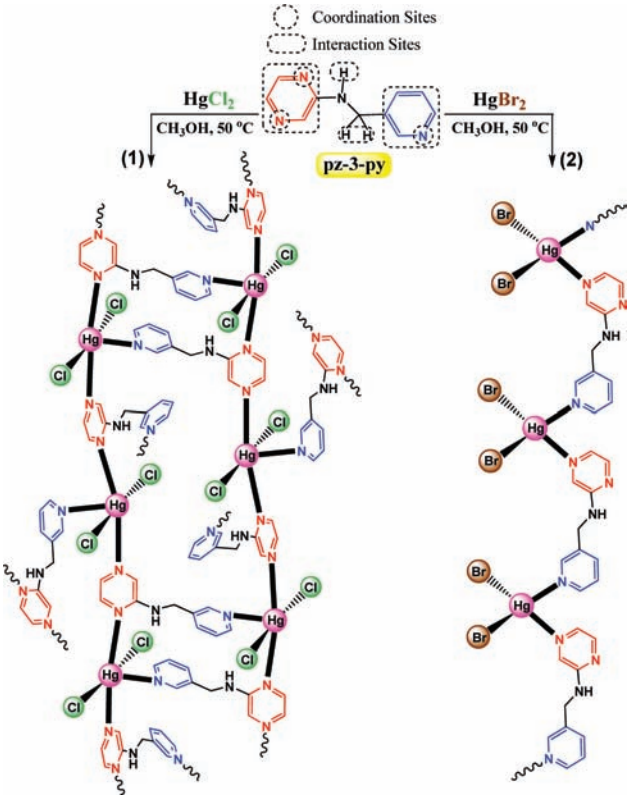

compounds. Dunbar and her co-workers[5h,i] have shown that discrete anions act as templates through noncovalent interactions and affect the outcome of the self-assembly process. Moreover, there are some reports that discuss the effect of coordinated anions on the structure of coordination compounds through the influence of noncovalent interactions.[5j,k] Since the role of the anion has emerged as an important consideration in engineering new supramolecular materials,[5h−m] we turned our attention to the effect of polarized metal-bonded anion interactions which can control the architecture of the final products. We have now designed a new flexible ligand with multiple coordination sites and also various interaction sites with diverse electronic properties (Scheme 1). Furthermore, choosing a labile metal which lacks strong coordination preferences such as Hg(II) provides us an opportunity to study how noncovalent interactions affect the self-assembly process and the architecture of the final products.[7]

In this contribution, we present the architectural control in two coordination polymers which have resulted from the self-assembly of HgX_2 (X = Cl, Br) and a new pyrazine−pyridine ligand (pz-3-py) under the same reaction conditions (Scheme 1). We have shown that by exploring noncovalent interactions through coordinated anions, a 2D network and a 1D zigzag chain were constructed for **1** and **2**, respectively.

Results and Discussion

Synthesis. pz-3-py was prepared as a yellow viscous oil from the reaction of 2-aminopyrazine and pyridine-3-aldehyde in a refluxing alcoholic solution in the presence of formic acid. This oil was used without further purification for complex synthesis. The treatment of mercury(II) halides (Cl, Br) with pz-3-py in methanol at 50 °C followed by slow evaporation of the solvent resulted in light yellow crystals of **1** (63% yield) and light orange crystals of **2** (45% yield) after a few days (Scheme 1). Unfortunately, our attempts to isolate a single crystal of mercury(II) iodide with pz-3-py were not successful until now, and we obtained an orange gel as a product.

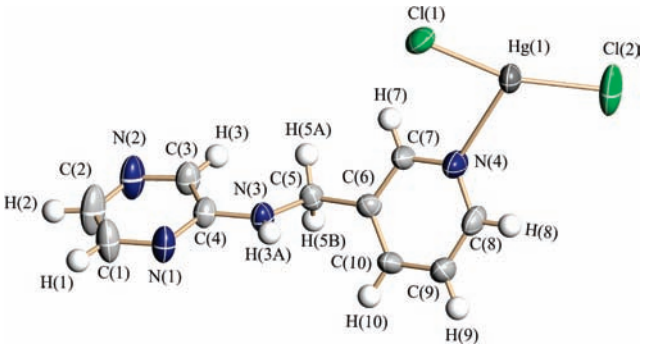

Figure 1. ORTEP of the crystallographically independent unit of **1** with the numbering scheme. Thermal ellipsoids are at the 50% probability level.

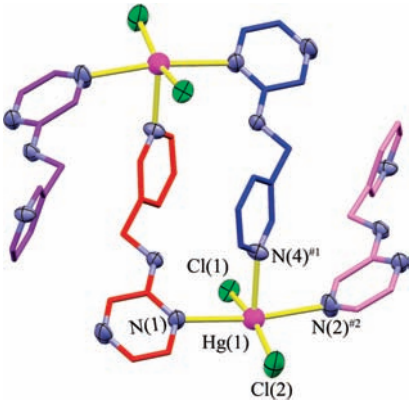

Figure 2. Plot showing the coordination sphere of Hg(II) in **1**. Nitrogen and chloride atoms are shown as ellipsoids (50% probability level) and metal centers as balls. Also, each pz-3-py ligand is represented in a different color for better demonstration, and hydrogen atoms were omitted for clarity. Symmetry codes: #1: $-x, -y, -z$. #2: $x, 1/2 - y, 1/2 + z$.

Crystal Structures and Noncovalent Interaction Analysis of 1 and 2. X-ray crystallographic analysis reveals that there is one Hg-pz-3-py moiety in the asymmetric unit of **1**[8a] (Figure 1). The Hg(II) ion is five-coordinated, and the coordination geometry for Hg^{2+} is a distorted square pyramid, with trigonality index[9] $\tau = 0.141$. The square plane is made up of two pyrazine nitrogens and two chlorine atoms, and the axial site is occupied by the pyridine nitrogen atom (Figure 2). Selected bond distances and angles for **1** are listed in Table 1. The Hg−N bond distance is 2.483(9) Å for $N(4)^{\#1}$ ($N_{pyridine}$), and

(7) Morsali, A.; Masoomi, Y. *Coord. Chem. Rev.* **2009**, *253*, 1882–1905.

(8) (a) Crystal data for **1**: $C_{10}H_{10}N_4Hg_1Cl_2$, fw = 457.71, monoclinic, space group $P2_1/c$, a = 11.0005(7) Å, b = 8.8159(7) Å, c = 15.8694(12) Å, β = 101.002(6)°, V = 1510.72(19) Å^3, Z = 4, D_{calc} = 2.012 g cm^{-3}, μ(Mo Kα) = 10.526 mm^{-1}, T = 298(2) K, crystal size = 0.50 × 0.49 × 0.20 mm, R1 = 0.0720, wR2 = 0.1992, GOF = 1.064 with $I > 2\sigma(I)$, CCDC 765612. (b) Crystal data for **2**: $C_{10}H_{10}N_4Hg_1Br_2$, fw = 546.61, monoclinic, space group $P2_1/a$, a = 9.3960(6) Å, b = 15.6032(7) Å, c = 10.0489(7) Å, β = 94.957(5)°, V = 1467.74(15) Å^3, Z = 4, D_{calc} = 2.474 g cm^{-3}, μ(Mo Kα) = 15.916 mm^{-1}, T = 120(2) K, crystal size = 0.25 × 0.24 × 0.15 mm, R1 = 0.0838, wR2 = 0.2243, GOF = 1.039 with $I > 2\sigma(I)$, CCDC 765611.

(9) Addison, A. W.; Rao, T. N.; Reedjik, J.; Van Rijn., J.; Verschorr, G. C. *J. Chem. Soc., Dalton Trans.* **1984**, 1349–1356.

Table 1. Selected Bond Distances (Å) and Bond Angles (deg) for **1** and **2**

1[a]		**2**[b]	
Hg(1)−N(1)	2.783(10)	Hg(1)−N(1)$^{\#1}$	2.496(9)
Hg(1)−N(2)$^{\#2}$	2.701(11)	Hg(1)−N(4)	2.419(11)
Hg(1)−N(4)$^{\#1}$	2.483(9)	Hg(1)−Br(1)	2.4713(14)
Hg(1)−Cl(1)	2.343(3)	Hg(1)−Br(2)	2.465(13)
Hg(1)−Cl(2)	2.323(3)	N(4)−Hg(1)−Br(1)	100.05(2)
Cl(1)−Hg(1)−Cl(2)	161.54(16)	N(4)−Hg(1)−N(1)$^{\#1}$	92.7(3)
Cl(2)−Hg(1)−N(4)$^{\#1}$	108.06(3)	N(4)−Hg(1)−Br(2)	98.7(2)
Cl(1)−Hg(1)−N(4)$^{\#1}$	89.9(2)	Br(1)−Hg(1)−Br(2)	154.59(6)
Cl(2)−Hg(1)−N(2)$^{\#2}$	91.0(2)	Br(2)−Hg(1)−N(1)$^{\#1}$	97.0(2)
Cl(1)−Hg(1)−N(2)$^{\#2}$	91.7(2)	Br(1)−Hg(1)−N(1)$^{\#1}$	98.4(2)
N(1)−Hg(1)−N(2)$^{\#2}$	169.99(5)		
N(1)−Hg(1)−N(4)$^{\#1}$	85.11(6)		
N(4)$^{\#1}$−Hg(1)−N(2)$^{\#2}$	85.0(4)		
Cl(1)−Hg(1)−N(1)	89.42(7)		
Cl(2)−Hg(1)−N(1)	91.07(6)		

[a] Symmetry codes: #1: $-x, -y, -z$. #2: $x, 1/2 - y, 1/2 + z$. [b] Symmetry code: #1: $x, y, -1 + z$.

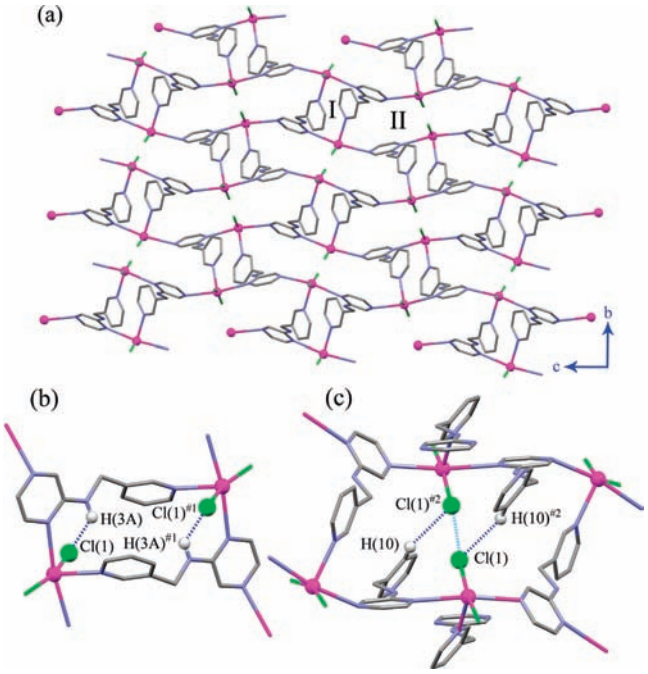

Figure 3. (a) A 2D sheet-like net in **1** along the *bc* plane containing boxes I and II. (b) N−H···Cl−Hg hydrogen bond represented by deep blue dashed lines in box I and (c) C−H···Cl−Hg hydrogen bond represented by deep blue dashed lines and Cl···Cl contact represented by light blue dashed line in box II. Noninteracting hydrogen atoms were omitted for clarity. Symmetry codes: #1: $-x, -y, -z$. #2: $-x, 1 - y, -z$.

longer distances were observed for pyrazine nitrogens according to 2.701(11) and 2.783(10)Å for N(2)$^{\#2}$ and N(1), respectively. Although the Hg−N bond distances for $N_{pyrazine}$ are a little longer than those for pyridine, they are in the range of coordination for the Hg−N bond.[10]

In compound **1**, pz-3-py acts as a μ_3-bridging ligand, and this compound represent 2D sheet-like networks parallel to the *bc* plane (Figure 3a). These sheets are formed by 16-membered $[M_2(pz\text{-}3\text{-}py)_2]$ metallacycles and 28-membered $[M_4(pz\text{-}3\text{-}py)_4]$ metallacycles, represented in Figure 3a as box I and box II, respectively. Polar metal−halogen bonds are good hydrogen bond acceptors, and the relative strength

(10) Dong, Y-.B.; Smith, M. D.; zur Loye, H.-C. *Solid State Sci.* **2000**, *2*, 861–870.

Table 2. Hydrogen Bond Parameters (Y−A···H−D) for **1** and **2**

D−H···A	D−H/Å	A···H/Å	A···D/Å	A···H−D/deg
compound **1**[a]				
N(3)−H(3A)···Cl(1)	0.86	2.85	3.476(10)	130
C(10)−H(10)···Cl(1)$^{\#2}$	0.93	2.84	3.513(10)	130
compound **2**[b]				
N(3)−H(3A)···N(2)$^{\#2}$	0.86	2.12	2.965(13)	165
C(5)$^{\#2}$−H(5B)$^{\#2}$···Cg2	0.97	2.79	3.67	150

[a] Symmetry code: #2: $-x, 1 - y, -z$. [b] Symmetry code: #2: $1/2 + x, 1/2 - y, z$. Cg2 = pyridine ring.

Scheme 2. Two Main Halogen···Halogen Interaction Type Geometries[13a]

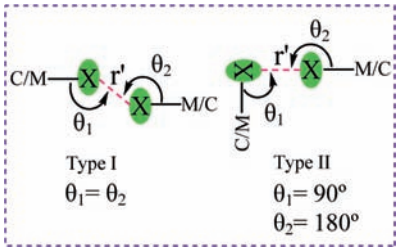

of the D−H···X−M hydrogen bonds lie in the order X = Cl ≥ Br for D = C, N, O.[11] This trend arises through the greater polarity of the M−Cl bonds compared to that of the M−Br bonds. The polarity of metal−halogen bonding is complicated by the increased electronegativity of Hg compared to lower atomic weight metals due to relativistic effects. This is the reason the HgX_2 unit is not dissociated into [HgX][X] salts. Also, the Hg−X bonds will have a substantial covalent component to the point that Br is likely to have very little polarity. According to this approach, there are moderate N−H···Cl−Hg and C−H···Cl−Hg hydrogen bonds acting as stabilizing noncovalent interactions in Figures 3b (box I) and c (box II), respectively. A summary of the hydrogen bond parameters for **1** is presented in Table 2.

Moreover, in compound **1**, there is also a short Cl···Cl contact (r' = 3.286(5) Å) in Figure 3c (box II) which is shorter than the sum of the van der Waals radii of Cl atoms (3.50 Å).[12] Two types of halogen···halogen interactions were defined, which have been summarized in Scheme 2.[13a] This halogen···halogen interaction belongs to type I, with an angle of Hg−Cl···Cl = $\theta_1 = \theta_2$ = 174.99(13)° (Scheme 2). Theoretical and crystallographical studies have shown that the type I of halogen···halogen interaction would be electrostatically repulsive.[13] It seems that this repulsive interaction along with the hydrogen bond has a structural controlling effect in compound **1**.

(11) (a) Aullón, G.; Bellamy, D.; Brammer, L.; Bruton, E. A.; Orpen, A. G. *Chem. Commun.* **1998**, 653–654. (b) Brammer, L.; Bruton, E. A.; Sherwood, P. *New. J. Chem.* **1999**, *23*, 965–968. (c) Brammer, L.; Bruton, E. A.; Sherwood, P. *Cryst. Growth Des.* **2001**, *1*, 277–290. (d) Brammer, L. *J. Chem. Soc., Dalton Trans.* **2003**, 3145–3157.

(12) Bondi, A. *J. Phys. Chem.* **1964**, *68*, 441–451.

(13) (a) Desiraju, G. R.; Parthasarathy, R. *J. Am. Chem. Soc.* **1989**, *111*, 8725–8726. (b) Price, S. L.; Stone, A. J.; Lucas, J.; Rowland, R. S.; Thornley, A. E. *J. Am. Chem. Soc.* **1994**, *116*, 4910–4918. (c) Day, G. M.; Price, S. L. *J. Am. Chem. Soc.* **2003**, *125*, 16434–16443. (d) Awwadi, F.; Willett, R. D.; Peterson, K. A.; Twamley, B. *Chem.—Eur. J.* **2006**, *12*, 8952–8960. (e) Zordan, F.; Brammer, L. *Cryst. Growth Des.* **2006**, *6*, 1374–1379. (f) Zordan, F.; Espallargas, G. M.; Brammer, L. *CrystEngComm* **2006**, *8*, 425–431.

An ORTEP view of the asymmetric unit of compound **2** is shown in Figure 4. Selected bond distances and angles for **2** are listed in Table 1. Interestingly, the structural analysis of **2**[8b] shows a remarkable architectural change in comparison with **1**, which is directed by an anion replacement from Cl to Br (Scheme 1). In contrast to **1**, the flexible pz-3-py acts as a μ_2-bridging ligand, and the Hg ion adopts a distorted tetrahedral geometry (Figure 5) through two nitrogens from pyrazine (Hg−N(1)$^{\#1}$ = 2.496(9) Å) and pyridine (Hg−N(4) = 2.419(11)Å) in a head-to-tail fashion and two bromide ions (Hg−Br(1) = 2.4713(14) Å; Hg−Br(2) = 2.4654(13) Å). As shown in Figure 6, this arrangement generates a 1D zigzag chain which is extended across the *c* axis. These chains are interlinked across the *a* axis by N−H···N and C−H···π hydrogen bonds (Figure 6a). A summary of geometric parameters of the hydrogen bonds for **2** are presented in Table 2. Moreover, the effective factor for the architectural versatility of **2** in comparison with **1** is the halogen···π interaction,[14] which is a well-known lone-pair−π interaction.[2e,f] This interaction is relatively rare but highly directional and effective in crystal packing. This type of noncovalent interaction forms between an electron-rich atom and an electron-poor π ring.[2e] As we know from halogen bonding theory, the polarizability and anisotropic character of the halogen atom increases from F to I.[2g] Hence, it is more convenient for Br than Cl to function as an electron-rich site on forming a lone-pair−π interaction at its equator region with electron-deficient rings. We explored the possibility that chains are also interlinked by a mutual halogen···π interaction across the *b* axis formed by the Br atom and the more electron-deficient pyrazine ring as a structure-directing factor in **2** (Figure 6b).

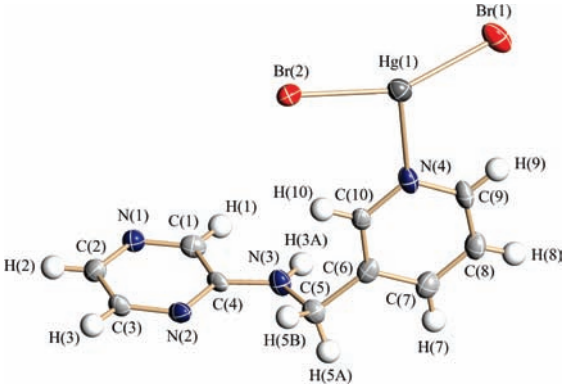

Figure 4. ORTEP of the crystallographically independent unit of **2** with the numbering scheme. Thermal ellipsoids are at 50% probability level.

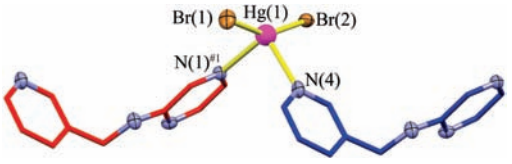

Figure 5. Plot showing the coordination sphere of Hg(II) in **2**. Nitrogen and bromide atoms are shown as ellipsoids (50% probability level) and metal centers as balls. Also, each pz-3-py ligand is represented in a different color for better demonstration, and hydrogen atoms were omitted for clarity. Symmetry code: #1: $x, y, -1 + z$.

Scheme 3 shows geometric parameters of the halogen···π interaction and also summarizes the halogen···π interactions classified as localized, semilocalized, and delocalized.[14b] The geometric parameters of two symmetry related Hg−Br···π interactions according to Scheme 3 are $D_{centroid}$ = 3.501(5) Å, d_{plane} = 3.37 Å, $r_{C(4)-N(2)}$ = 3.39 Å, d_{offset} = 0.94 Å,

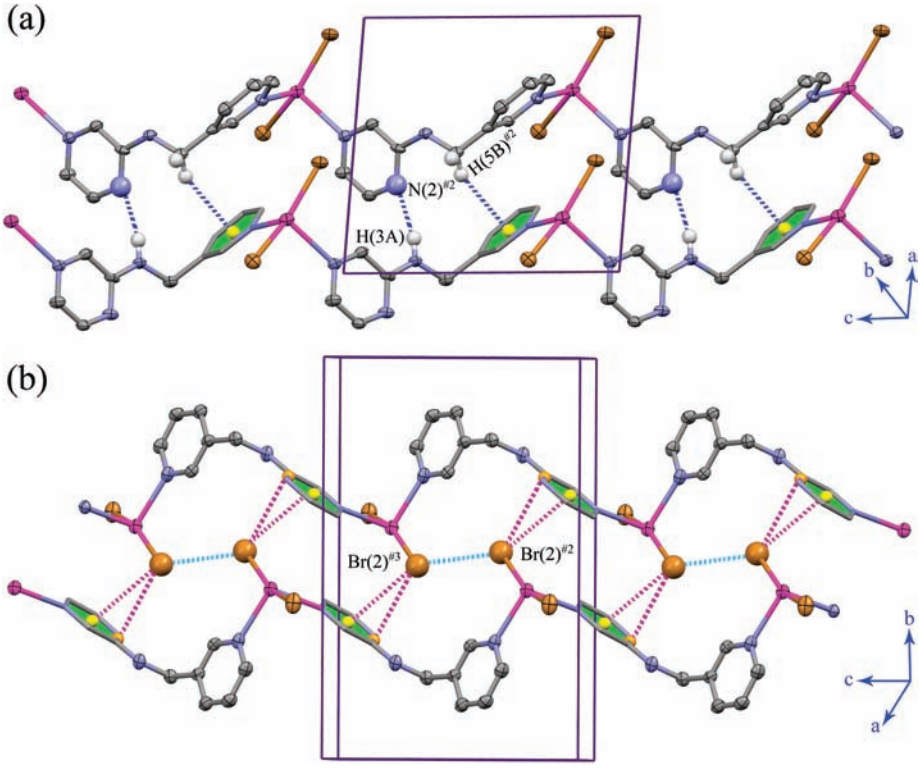

Figure 6. (a) N−H···N and C−H···π hydrogen bonds between chains in **2** across the *a* axis. (b) Hg−Br···π interaction and also Br···Br contact between chains in **2** across the *b* axis. Symmetry codes: #2: $1/2 + x, 1/2 - y, z$. #3: $1/2 - x, 1/2 + y, 1 - z$.

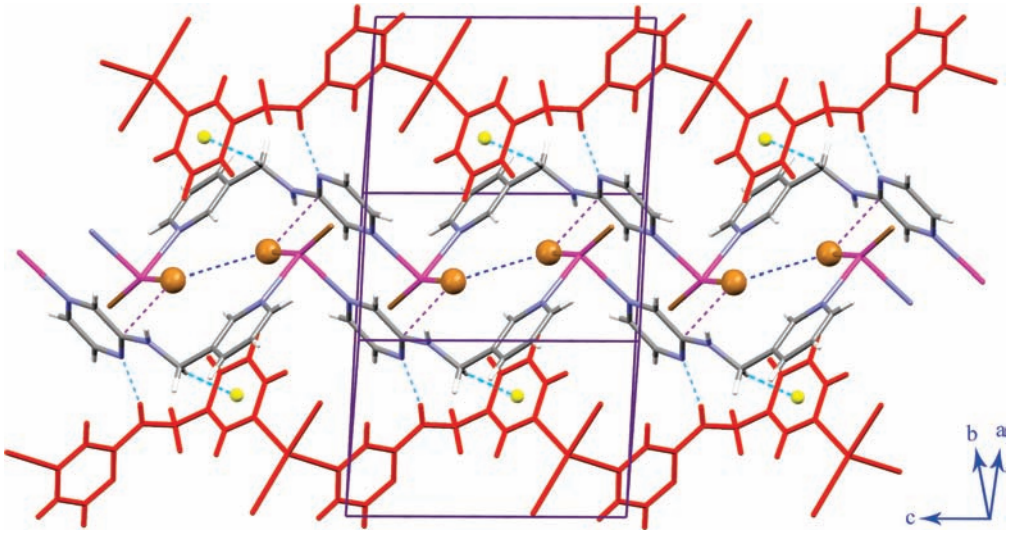

Figure 7. Packing view of **2** showing cooperative noncovalent interactions (dash lines) between 1D zigzag chains.

Scheme 3. (Left) Geometric Parameters of Halogen···π Interactions[a] and (Right) Halogen···π Classification[14b,b]

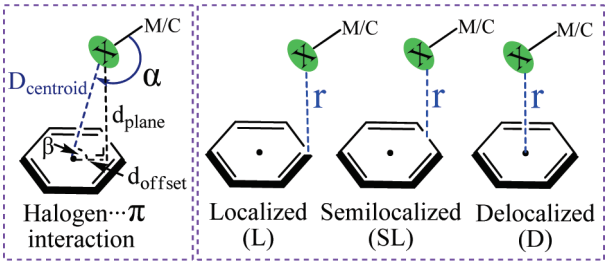

[a] $D_{centroid}$ is the halogen distance from the centroid of ring atoms. d_{palne} is the normal line from the halogen to the ring plane. d_{offset} is the parameter which determines dispalacement of the halogen from the center of the aromatic ring [$d_{offset} = (D_{centroid}^2 - d_{plane}^2)^{1/2}$]. [b] r is the shortest distance between the halogen and ring member atom, bond, or centroid of the ring atoms.

$\alpha = 88.50(8)°$, and $\beta = 74.3°$. So, these interactions are categorized as a relatively strong[2e] semilocalized (SL) type.[14b] A simple survey in the CSD[15] (with the help of ConQuest version 1.12) shows that the Hg−X···π interaction is not rare but has been overlooked in most cases because of the existence of other interactions. An interesting example was reported by Puddephatt and Burchell[16] in which excess mercury salts acted as a template for macrocyle formation through Hg−Br···π and Hg−I···π (CSD refcodes: JAPKER and JAPKIV).

Furthermore, in compound **2**, there is also a short Br···Br contact between chains across the *b* axis (Figure 6b) with $r' = 3.5926(19)$ Å, which is shorter than the sum of the van der Waals radii of Br atoms (3.7 Å).[12] This halogen···halogen interaction belongs to type I with angle of Hg−Br···Br = $\theta_1 = \theta_2 = 123.82(3)°$ (Scheme 2).[13a] As mentioned before, studies have shown that the type I of halogen···halogen interaction would be electrostatically repulsive.[13] So, cooperative hydrogen bond and halogen···π interactions presumably overcome this repulsive interaction and also act as architectural controlling factors in compound **2**. We present the packing diagram of compound **2** in Figure 7. Cooperative noncovalent interactions such as N−H···N_{pz} and C−H···π_{py} hydrogen bonds (light blue dashed lines), Hg−Br···π_{pz} interactions (purple dashed lines), and Br···Br contacts (deep blue dashed lines) are shown in Figure 7, and they act coherently as structure directing factors in compound **2**.

Conclusion

In conclusion, we have described the self-assembly of HgX_2 (X = Cl, Br) and a new pyrazine−pyridine ligand under the same reaction conditions. In the case of compound **1**, the 2D network was constructed by moderate noncovalent interactions such as N−H···Cl−Hg and C−H···Cl−Hg hydrogen bonds and also type I of Cl···Cl contacts. While the coordinated bromide anions play different roles in compound **2**. In compound **2**, a remarkable architectural change from the 2D network seen in compound **1** to a 1D zigzag chain in **2** took place. We have shown that through anion replacement from Cl to Br, cooperative noncovalent interactions such as N−H···N and C−H···π hydrogen bonds, Hg−Br···π interactions, and Br···Br contacts act coherently as structure directing factors in compound **2**. Our results show that coordinated anions can control the architecture and topology of final products in the self-assembly process by choosing more favorable noncovalent interactions in a cooperative manner.

Experimental Section

Materials and Instruments. All reagents and solvents were purchased from chemical sources and were used directly without further purification. UV−vis spectra were recorded on a Shimadzu 2100 spectrometer using a 1-cm-path-length cell. Infrared spectra (4000−250 cm^{-1}) of solid samples were taken as a 1% dispersion in CsBr pellets using a Shimadzu-470 spectrometer. Elemental analysis was performed using a Heraeus CHN-O Rapid Analyzer. Melting points are uncorrected and were obtained by an Electrothermal 9100 melting point apparatus.

(14) (a) Reddy, D. S.; Craig, D. C.; Desiraju, G. R. *J. Am. Chem. Soc.* **1996**, *118*, 4090–4093. (b) Shishkin, O. V. *Chem. Phys. Lett.* **2008**, *458*, 96–100. (c) Yin, Z.; Wang, W.; Du, M.; Wang, X.; Guo, J. *CrystEngComm* **2009**, *11*, 2441–2446. (d) Schollmeyer, D.; Shishkin, O. V.; Rühl, T.; Vysotsky, M. O. *CrystEngComm* **2008**, *10*, 715–723.

(15) *Cambridge Structural Database*, version 5.30, November 2008; CCDC: Cambridge, U. K.

(16) Burchell, T. J.; Puddephatt, R. J. *Inorg. Chem.* **2005**, *44*, 3718–3730.

Caution! *The pz-3-py ligand vapors cause violent skin and eye irritation.*

Synthesis of N-(Pyridin-3-ylmethyl)pyrazin-2-amine (pz-3-py). 2-Aminopyrazine (1.944 g; 20.86 mmol) was dissolved in ethanol (25 mL) and mixed dropwise with pyridine-3-aldehyde (2 mL, 20.86 mmol). Formic acid (1 mL) was added to the reaction vessel, and the mixture was heated under reflux for 12 h. The solvent was removed by heating, and a yellowish, highly viscous oil was obtained as a product (3.8 g). UV−vis (DMSO, λ_{max}): 323, 261 nm.

Synthesis of [Hg(μ_3-pz-3-py)Cl_2]$_n$ (1). $HgCl_2$ (0.176 g, 0.648 mmol) was dissolved in methanol (20 mL) and mixed with pz-3-py (0.5 mL) in (10 mL) methanol. The mixture was stirred at 50 °C until the volume reduced to 20 mL. The solution was filtrated, and by slow evaporation of this solution at room temperature, light yellow crystals of **1**, which were also suitable for X-ray analysis, were formed after one week (yield 0.187 g, 63%, mp 244−245 °C decompose). Anal. Calcd for $C_{10}H_{10}N_4Cl_2Hg_1$ (%): C, 26.24; H, 2.20; N, 12.24. Found: C, 26.20; H, 2.15; N, 12.19. IR (CsBr, cm^{-1}): 3312 (w), 1593 (s), 1547 (m), 1512 (s), 1426 (s), 1327 (s), 1275 (m), 1198 (m), 1143 (m), 1065 (s), 1004 (w), 957 (w), 896 (w), 830 (m), 775 (w), 712 (m), 624 (w), 594 (w), 420 (m), 323 (w), 276 (w).

Synthesis of [Hg(μ-pz-3-py)Br_2]$_n$ (2). The procedure was similar to the synthesis of **1** except that $HgBr_2$ (0.233 g, 0.646 mmol) was used instead of $HgCl_2$. Light orange crystals of **2** were formed on slow evaporation of the filtrate at room temperature over one week (yield 0.159 g, 45%, mp 195−198 °C decompose). These crystals were suitable for X-ray analysis. Anal. Calcd for $C_{10}H_{10}N_4Br_2Hg_1$ (%): C, 21.97; H, 1.84; N, 10.25. Found: C, 21.76; H, 1.65; N, 10.31. IR (CsBr, cm^{-1}): 3251 (m), 1602 (s), 1521 (s), 1479 (m), 1429 (m), 1400 (m), 1347 (m), 1272 (m), 1210 (m), 1182 (w), 1146 (s), 1078 (s), 1050 (m), 1003 (m), 962 (m), 907 (w), 858 (w), 832 (m), 811 (m), 754 (w), 712 (m), 649 (m), 567 (w), 540 (w), 422 (m), 375 (w).

Crystal Structure Determination and Refinement. The X-ray diffraction measurements were made on a STOE IPDS-II diffractometer with graphite monochromated Mo Kα radiation. For [Hg(μ_3-pz-3-py)Cl_2]$_n$ (**1**), light yellow block-shaped and, for [Hg(μ-pz-3-py)Br_2]$_n$ (**2**), light orange block-shaped crystals were chosen using a polarizing microscope and were mounted on a glass fiber which was used for data collection. Cell constants and orientation matrices for data collection were obtained by least-squares refinement of diffraction data from 4008 unique reflections for **1** and 3948 unique reflections for **2**. Data were collected to a maximum 2θ value of 58.50° for **1** and to a maximum 2θ value of 58.56° for **2**, in a series of ω scans in 1° oscillations and integrated using the Stoe X-AREA[17] software package. A numerical absorption correction was applied using the X-RED[18] and X-SHAPE[19] software. The data were corrected for Lorentz and polarizing effects. The structures were solved by direct methods[20] and subsequent difference Fourier maps and then refined on F^2 by a full-matrix least-squares procedure using anisotropic displacement parameters.[20] All hydrogen atoms in **1** and **2** were added at idealized positions. The atomic factors were taken from the International Tables for X-ray Crystallography.[21] All refinements were performed using the X-STEP32 crystallographic software package.[22]

Acknowledgment. We would like to thank the Graduate Study Councils of Shahid Beheshti University, G. C. for their financial support.

Supporting Information Available: X-ray crystallographic data in CIF format and also tables of atomic coordinates, bond lengths, bond angles, and anisotropic displacement parameters for **1** and **2**. This material is free of charge via the Internet at http://pubs.acs.org.

(17) *X-AREA: Program for the Acquisition and Analysis of Data*, version 1.30; Stoe & Cie GmbH: Darmstadt, Germany, 2005.
(18) *X-RED: Program for Data Reduction and Absorption Correction*, version 1.28b; Stoe & Cie GmbH: Darmstadt, Germany, 2005.
(19) *X-SHAPE: Program for Crystal Optimization for Numerical Absorption Correction*, version 2.05; Stoe & Cie GmbH: Darmstadt, Germany, 2004.
(20) Sheldrick, G. M. *SHELX97*; University of Göttingen: Göttingen, Germany, 1997.
(21) *International Tables for X-ray Crystallography*, Vol. *C*; Kluwer Academic Publisher: Dordrecht, The Netherlands, 1995.
(22) *X-STEP32: Crystallographic Package*, version 1.07b; Stoe & Cie GmbH: Darmstadt, Germany, 2000.